


Nano Acacetin Mitigates Intestinal Mucosal Injury in Sepsis Rats by Protecting Mitochondrial Function and Regulating TRX1 to Inhibit the NLRP3 Pyroptosis Pathway

Ning-ke Guo^{1,*}, Li-ning Si^{1,2,*}, Pei-qing Li¹ , Gui-fen Gan²

¹Graduate School, Qinghai University, Xining, Qinghai, People's Republic of China; ²Affiliated Hospital, Qinghai University, Xining, Qinghai, People's Republic of China

*These authors contributed equally to this work

Correspondence: Gui-fen Gan, Email xzhd1991@163.com

Background: Acacetin (AC) is a flavonoid compound with antiperoxidant, anti-inflammatory, and antiplasmodial activity. However, the solubility of AC is poor and nano acacetin (Nano AC) was synthesized. The intestinal mucosal barrier is impaired in sepsis rats, and the protective effects and mechanism of AC and Nano AC on the intestinal mucosal barrier are unclear.

Methods: Cecal ligation and perforation (CLP) was used to induce sepsis in rats, and lipopolysaccharide (LPS)-stimulated intestinal epithelial cells were used to observe the effects of AC and our synthesized Nano AC on the amelioration of intestinal mucosal damage. The molecular docking technique was used to predict the binding energy of AC to thioredoxin reductase 1 (TRX1) signaling pathway proteins. TRX1 inhibitor (PX-12) was employed to elucidate the protective signaling pathway of Nano AC in LPS-stimulated intestinal epithelial cells.

Results: Our synthesized Nano AC, with an average particle size of 17.18 ± 0.48 nm and an uptake rate of 95% in intestinal epithelial cells. The maximum binding capacity of AC to TRX1 was -6.82 kcal/mol, supporting the hypothesis that TRX1 is a potential target of AC. AC and Nano AC ameliorated the survival rate, intestinal mucosal damage score, pathological morphology, hepatic and renal function, and myocardial troponin levels, decreased serum levels of pyroptosis-related factors, upregulated TRX1, down-regulated NOD-like receptor protein 3 inflammasome (NLRP3), cysteinyl aspartate specific proteinase-11 (Caspase-11), Gasdermin D (GSDMD) in sepsis rats. They improved mitochondrial morphology and mitochondrial reactive oxygen species (ROS) levels, reduced pyroptosis levels, and upregulated TRX1, which adjusted NLRP3/ Caspase-11/ GSDMD signaling pathway in LPS-stimulated intestinal epithelial cells. Moreover, Nano AC was more effective.

Conclusion: AC and Nano-AC can inhibit the NLRP3/Caspase-11/GSDMD signaling pathway by upregulating TRX1 to ameliorate intestinal mucosal injury in sepsis rats, and the effect of Nano AC is more prominent.

Keywords: sepsis, nano AC, intestinal mucosal barrier, PX-12, pyroptosis

Introduction

Sepsis triggers a dysregulated host response to infection that harms the body as a systemic inflammatory response syndrome,^{1,2} which is induced by lipopolysaccharide (LPS).³ Globally, the number of sepsis patients has dramatically increased and is estimated to affect more than 30 million patients, causing nearly six million deaths annually.⁴ Sepsis can lead to severe immune dysfunction, ileus, and even death.^{5,6} Intestinal barrier damage is a common phenomenon in patients with sepsis, which plays a crucial role in the development and deterioration of sepsis.⁷ The intestinal tract has been described as the engine of sepsis, and disruption of the intestinal barrier may increase the incidence of fatal sepsis.⁸ Bacterial translocation occurs during this period, inducing an inflammatory response,⁹ and the intestinal mucosal barrier

prevents microorganisms from entering the intestinal tract from the bloodstream. Excessive inflammation damages the intestinal epithelium, leading to a compromised intestinal mucosal barrier that promotes bacterial migration and toxin dissemination.¹⁰ Thus, a comprehensive understanding of inflammation is essential for elucidating the mechanisms underlying intestinal barrier dysfunction and developing more effective treatments for sepsis.

Acacetin (5,7-dihydroxy-40-methoxyflavone) is an O-methylated flavonoid monomer and a biologically active constituent found in a variety of plants, including *Sparganii rhizoma*, *Sargentodoxa cuneata*, and *Patrinia scabiosifolia*.¹¹ Acacetin (AC) possesses antiperoxidant, anti-inflammatory, and antiplasmodial activity, with a molecular weight of 284.26 and chemical formula C₁₆H₁₂O₅. AC is reported for the anti-microbial activity against different types of microbes and possessed anti-bacterial activity against clinically isolated Methicillin-resistant *Staphylococcus aureus*.^{12,13} Moreover, AC has been reported to exhibit significant anti-inflammatory effects.¹⁴ In vivo studies, AC prevented d-galactosamine (GalN)/LPS-induced liver injury by inhibiting the TLR4 signaling pathway.¹⁵ In vitro studies, AC inhibited LPS-induced upregulation of inducible nitric oxide synthase (iNOS) and cyclooxygenase 2 (COX-2) in macrophages and 12-O-tetradecanoylphorbol-13-acetate (TPA)-induced tumor initiation in mice.¹⁶ Some studies have shown that AC inhibits sepsis-induced acute lung injury through its anti-inflammatory and antioxidant activities.¹⁷ However, the effect and mechanism of AC on septic intestinal damage remains unclear.

Compared to flavonoids, AC possesses poor water solubility (64.4±10.9 ng/mL), limited ethanol solubility (0.712±0.002 mg/mL), and very low oral bioavailability.¹⁸ The rapid development of nanotechnology is noteworthy. Currently, some studies have focused on nanocarriers composed of proteins, which are promising colloidal drug delivery systems for delivering bioactive payloads and nutraceuticals.^{19,20} Other carriers such as, chitosan are modified with a wide range of compounds owing to bonding with acetamido, hydroxyl, and amine sites.²¹ In this study, zein carriers are employed, which is a plant protein extracted from corn to form a gastro-resistant and mucous membrane-linked polymer, and is cheap and readily available and facilitates packaging with a bioactive substance that possesses hydrophilic, hydrophobic, and amphiphilic traits.²² Zein can easily self-assemble into nanoparticles with various structures, depending on the solvent and assembly conditions.²³ In addition, transferrin receptors on the surface of intestinal epithelial cells can promote nanoparticle uptake by intestinal epithelial cells.²⁴ Previous studies have found that zein is used as a carrier by tyrosine protein kinase receptor B agonists, improving their therapeutic effects in Alzheimer's disease. Moreover, zein has been used for packaging hydrophobic compounds, such as curcumin, resveratrol, and so on, which significantly increases the bioavailability of these compounds.²⁵ The unique advantages of zein make it a promising research subject. In this study, zein was employed to synthesize Nano AC by observing its protective effect against the intestinal mucosa of sepsis rats in vivo and in vitro and further exploring the underlying mechanisms.

Pyroptosis is a specific pro-inflammatory form of programmed cell death that is dependent on the enzymatic activity of the cysteine-dependent aspartate-specific protease (caspase) family.²⁶ Pyroptosis is mediated by some caspase family proteins that activate the inflammatory cytokines interleukin 1 β (IL-1 β) and IL-18. Cellular pyroptosis is accomplished by gasdermin D (GSDMD), which is cleaved by caspases 1, 4, 5, and 11 to form N-terminal fragments.²⁷ Subsequently, a pore is formed at the plasma membrane of GSDMD-N, releasing mature IL-1 β and IL-18.²⁸ Increased levels of cellular pyroptosis play a crucial role in the development of sepsis.^{29,30} A previous study reported that reactive oxygen species (ROS) production can occur via cellular pyroptosis in damaged mitochondria.³¹ Mitochondrial ROS (mtROS) are one of the most essential pro-inflammatory signals that can be scavenged by mitochondrial thioredoxin (TRX) antioxidants, and inflammatory activation disrupts the integrity of mitochondria.³² The protective effect of AC on the mitochondria has been previously reported. For example, AC pretreatment significantly ameliorated mitochondrial membrane potential dysfunction.³³ However, the mechanism by which AC protects mitochondrial function and inhibits cellular pyroptosis by regulating TRX1 remains unclear. Among the TRX family members, TRX1 is frequently studied, not only because TRX1 serves as a key component of redox regulation but also because it is critical for growth promotion, inflammation regulation, and anti-apoptosis. Increased levels of TRX1 may promote cell growth and proliferation, which plays a role in many human diseases.³⁴ Inflammasomes are a group of cytoplasmic protein complexes that form the basis for various diseases.³⁵ The NOD-like receptor protein 3 (NLRP3) inflammasome is required for activation of caspase 11.³⁶ Recent studies have shown that NLRP3 inflammatory vesicle-associated pyroptosis plays a vital role in intestinal diseases, particularly dextran sodium sulfate (DSS)-induced colitis and inflammatory bowel disease.³⁷ Previous studies have

suggested the activation of the NLRP3 inflammasome by TRX1 knockdown in a rat model of middle cerebral artery occlusion.³⁸ However, the mechanism through which TRX1 regulates NLRP3 pyroptosis pathway in sepsis rats remains unclear.

Materials and Methods

Ethical Approval of the Study Protocol

The study protocol was approved by the Ethics Committee of the Clinical School of Medicine of Qinghai University (Xining, China; approval number: P-SL-2024-003). The study conformed to the Guide for the Care and Use of Laboratory Animals published by the US National Institutes of Health (8th edition, 2011, National Institutes of Health, Bethesda, MD, USA).

Reagent

Lipopolysaccharide (LPS) (Cat.L8274), zein (Cat.Z3625), and Adenosine-triphosphate (ATP) (Cat.A2383-5G) were purchased from Sigma company (USA). Acacetin (Cat.GC71983) was purchased from InnoChem company (China), ELISA kits of Interleukin-1 β (IL-1 β) (Cat.E-EL-R0012), Interleukin-18 (IL-18) (Cat.E-EL-R0567), D-lactic acid (Cat. E-BC-K002-M), Aspartate aminotransferase (AST) (Cat. E-BC-K236-M), Alanine aminotransferase (ALT) (Cat. E-BC-K235-M), Creatinine (Crea) (Cat. E-BC-K188-M), Urea nitrogen (Urea) (Cat. E-BC-K183-M), Cardiac troponin T (cTnT) (Cat. E-EL-R0151) and Cardiac troponin I (cTnI) (Cat. E-EL-R1253) were purchased from Elabscience company (China). Marker (Cat.PM2510) was purchased from SMOBIO company (China). Antibodies for Thioredoxin 1 (Cat. 2429S), β -actin (Cat. 4967S), and Caspase11 (Cat. 143140S) were purchased from Cell Signaling Technology company (USA), antibodies for NLRP3 (Cat. MA532255) was purchased from Invitrogen company (USA), antibodies for Gasdermin D (Cat.PD00-18) was purchased from HUABIO company (China). Peroxidase AffiniPure Goat Anti-Rabbit IgG (Cat.DY60202) and Cell Counting Kit-8 (CCK-8) (Cat.DY40201) were purchased from DEEYEE company (China). Peroxidase AffiniPure Goat Anti-Rat IgG (Cat.SE132) and DAPI (Cat. C0065) were purchased from Solarbio company (China). Ultra-sensitive ECL Reagent (Cat.DY30208) and MitoTracker Green (Cat.DY50401) were purchased from DEEYEE company (China). MitoSOX Red (Cat. HY-D1055), Fluorescence secondary antibody (Cat. HY-P8002), and PX-12 (Cat. HY-13734) were purchased from MedChemExpress (USA). Closed with normal sheep serum (Cat. ZLI-9022) and DAB color development solution (Cat. ZLI-9018) were purchased from Nakasugi Golden Bridge company (China). Intestinal epithelial cell lines were obtained from Beijing Beina Chuanglian Biotechnology Research Institute (China). Dulbecco's Modified Eagle Medium (DMEM) (Cat.10-013-CVRC) and trypsin (Cat.25-053-CL) were purchased from CORNING company (China). Penicillin-streptomycin was purchased from MedChemExpress (USA).

Preparation of Nano AC

Using 80% ethanol as the solvent, 10 mg/mL zein solution was prepared. AC and ethanol were equally mixed and stirred at constant temperature for 20 min. Then, the solution was poured into a 50 mL spray bottle (with droplet sizes of approximately 10–50 μ m), and another equivalent of deionized water was poured into another spray bottle (with a droplet size of approximately 10–50 μ m). The two spray bottles were sprayed to obtain a large amount of milky yellow liquid in a closed device, and the drug-carrying zein nanoparticles and ethanol were removed by rotary evaporation and ultrasonication for 20 min.³⁹

Characterization of Nano AC

Liquid chromatography-mass spectrometry (LCMS) was used to characterize the Nano AC. According to the energy-level transition caused by the absorption of the radiation energy, the infrared absorption spectrum of the molecule was obtained by recording the transition process (infrared spectroscopy). Transmission electron microscopy was used to characterize the appearance of the drug-loaded zein nanoparticles. Nanoparticle size, zeta potential (ZP), and polydispersity index (PDI) were measured using a nanoparticle size and zeta potential analyzer at 25°C.

Determination of Nano AC Encapsulation Efficiency and Drug Loading

3 mL Nano AC was centrifuged at 12000 r/min for 30 min, and then the free AC content was detected in the supernatant (W_1); 3 mL Nano AC was filtered through a microporous filter membrane (0.45 μm), which was injected into chromatography to analyze as WT; 100 μL Nano AC was added into 4900 μL 80% ethanol, and ultrasonicated for 30 min. The content was detected (W_2), and the total mass was obtained by freeze-drying 1 mL of Nano AC (W). The encapsulation rate and drug loading were calculated according to the formulas: encapsulation rate = $(WT - W_1)/WT \times 100\%$, drug loading = $W_2/W \times 100\%$. The chromatographic column conditions were as described above.

Uptake Percentage of AC and Nano AC

The organic phase was prepared by adding approximately 8 mg rhodamine B, with homogenous preparation, and the precipitates were washed with distilled water to remove free rhodamine B. Rhodamine B-containing AC and Nano AC 10 $\mu\text{mol/L}$ were added after the intestinal epithelial cells in the culture plate were pre-cultured for adherent growth, and the cells were rinsed twice with PBS after incubation for 10 min, 30 min, 60 min, 120 min, and 240 min. After trypsin digestion, the cells were collected and the fluorescence intensity of the cell suspensions was measured using an enzyme labeling instrument at a wavelength of 485 nm. Percentage of uptake (%) = $M/M_0 \times 100\%$, where M is the fluorescence intensity of the cell suspension measured at different sampling times and M_0 is the initial fluorescence intensity added to the cell suspension. When trypsin was not added, the fluorescence intensity was observed using a laser confocal microscope.⁴⁰

Establishment of Sepsis Model

Adult SD rats (weight, 200–220) g were provided by Qinghai University, and animal husbandry and experimental procedures followed the regulations of the Committee on Animal Ethics. SD rats were anesthetized by intraperitoneal injection of sodium pentobarbital (45 mg/kg), sterilized, and disinfected by incision of the peritoneal cavity, removal of the cecum, rolling of feces to the end, tying the fecal ligature with silk threads, piercing the end of the cecum to 0.7 cm with a cone, returning the cecum to the abdominal cavity, suturing the wound, injecting 5 mL of saline intraperitoneally, and returning to the cage for any water or food. When MAP was decreased to 70 mmHg or 30%, the model of sepsis was successfully established, and subsequent experiments could be performed.⁴¹ Cecal ligation and perforation (CLP) rats were lethargic and lacked interest in the environment, with erect hair and crusty exudates around the eyes. CLP rats did not receive any antibiotic treatment because they may have had altered intestinal inflammation.⁴²

Experimental Protocol

In vivo Experiments

80 SD rats were divided into five groups according to the random sampling method: sham operation (Sham) group, non-nanoparticle (Non-nano) group, sepsis (Sep) group, acacetin (AC) group, and nano acacetin (Nano AC) group. Sham group: only open and closed abdomen; Non-nano group: non-nanoparticle has the same synthetic process as Nano AC without AC. Open and closed abdomen, then 50 mg/kg non-nanoparticle was intraperitoneally injected; Sep group: cecum ligation and perforation (CLP) to create a sepsis model; AC group: before establishment of CLP, 5 mg/kg acacetin was intraperitoneally injected, and 12 h after CLP, 5 mg/kg acacetin was intraperitoneally injected again. Nano AC group was injected with the same dose and method as AC group. 16 rats in each group were used to observe survival time and survival rate. In subsequent experiments, 32 SD rats were divided into four groups by random sampling method: Sham group, Sep group, AC group, Nano AC group, and 8 rats in each group. They were used to detect IL-1 β , IL-18, and blood D-lactate levels; the expression of intestinal tissue TRX1, NLRP3, Caspase11, and GSDMD; intestinal mucosal damage fraction; intestinal pathomorphology; and changes in cardiac troponin, liver, and kidney functions.

In vitro Experiments

Cells were cultured in a humidified incubator at 37°C, 95% air, and 5% CO₂. DMEM was supplemented with 10% fetal bovine serum (v/v). The cells were cultured with 100 U/mL penicillin and 100 $\mu\text{g/mL}$ streptomycin. Intestinal epithelial cells were taken after 3–5 generations of treatment and divided into control (Control) group, Non-nano

group, LPS group, AC group, and Nano AC group. Control group: the culture medium was changed to serum-free basal medium 12 h before the experiment; Non-nano group: the cells were incubated with serum-free basal medium by adding 100 $\mu\text{mol/L}$ non-nano. LPS group: the cells were incubated with serum-free basal medium by adding 1 $\mu\text{g/mL}$ LPS for 12 h, and then with 5 mmol/L adenosine-triphosphate (ATP) for 2 h; AC group: the cells were incubated with serum-free basal medium by adding 10 $\mu\text{mol/L}$ AC and 1 $\mu\text{g/mL}$ LPS for 12 h, then 5 mmol/L ATP and 10 $\mu\text{mol/L}$ AC were added and incubated for 2 h. Nano AC group: The cells were incubated with serum-free basal medium by adding 10 $\mu\text{mol/L}$ Nano AC and 1 $\mu\text{g/mL}$ LPS for 12 h, then 5 mmol/L ATP and 10 $\mu\text{mol/L}$ Nano AC were added, and incubated for 2 h. After drug interference, the supernatant was discarded, and the mitochondrial morphology was observed in each group. In subsequent experiments, cells were divided into Control group, LPS group, AC group, and Nano AC group. Mitochondrial ROS level and protein expression of TRX1, NLRP3, Caspase11, and GSDMD of intestinal epithelial cells were determined in each group; Then PX-12 group was added to the subsequent experiments: serum-free basal medium was added to the incubator for 12 h with 10 $\mu\text{mol/L}$ Nano AC, 1 $\mu\text{mol/L}$ PX-12, and 1 $\mu\text{g/mL}$ LPS, and then added to the incubator for 2 h with 5 mmol/L ATP and 10 $\mu\text{mol/L}$ Nano AC. The fluorescence expression, protein expression of NLRP3, GSDMD, and cell viability were determined in the respective groups.

Observation of Survival Rate in Rats

After intraperitoneal injection of drugs 12 h after CLP, the rats were returned to the cage, fed, and watered ad arbitrium, which were observed once 1 h for 48 h. The survival times and statuses of the rats were recorded.

HE Staining

SD rats intestinal segment of 6–7 cm was taken on ice, and fixed with 4% paraformaldehyde solution for 48–72 h. The tissues were cut into small pieces, dehydrated overnight, embedded in paraffin, sectioned on an ultrathin microtome, soaked in xylene for 8 min, rehydrated in different concentrations of ethanol for 3 min, and washed with tap water for 10 s. After rehydration, the intestinal tissue was stained in hematoxylin staining solution for 8 min, cleaned with tap water for 20 s, separated 1% hydrochloric acid alcohol color, washed with water for 10 s, reblued at 40 °C, transferred to eosin staining solution for 60 s, and washed the excess eosin dye with different concentrations of ethanol, sealed, dried, and then photographed under a light microscope in randomly selected areas.⁴³

HE Staining Was Observed to Grade the Intestinal Mucosal Damage Score

Grade 0: Normal mucosal villi; Grade 1: edema occurs in the Gruenhagen's space, usually with capillary congestion; Grade 2: moderate extension of the lymphatic interstitium and dilation of the subepithelial space; Grade 3: partial loss of villi with epithelial cells at the tip; Grade 4: Large amounts of epithelium elevated along the epithelium on both sides of the villi, except for exfoliation of the apex; Grade 5: separation of the epithelium and the membrane of the lamina propria has progressed from the tip toward the base, exposing one-third to one-half of the lamina propria, moderate vasodilatation, capillary congestion within the lamina propria, and terminal submucosa; Grade 6: Basic completion of complete loss of the epithelium, with exposure of the lamina propria, capillary dilatation, and increased cellular infiltration within the lamina propria; Grade 7: destruction and disintegration of the lamina propria, with hemorrhagic hemorrhage and ulceration.⁴⁴

Measurement of Blood Inflammatory Cytokines, Cardiac Troponin

After 12 h of CLP, the abdominal cavity was opened. 2 mL blood was extracted from the rat abdominal aorta and centrifuged at 1000 \times g for 20 min. According to the kit instructions, working solutions of biotinylated antibody, working solution of enzyme conjugate, substrate solution, and termination solution were added sequentially. The OD value was determined by enzyme labeling instrument, and the concentrations of IL-1 β , IL-18, cardiac troponin T (cTnT), and cardiac troponin I (cTnI) in the blood of each group of rats were calculated using a standard curve.

Measurement of Blood Liver Function

After 12 h of CLP, the same method as above, the upper layer of serum was taken, and the standard or sample was added to each well of enzyme plate. They were incubated at 37°C for 30 min, adding the color developer. After shaking and mixing on the enzyme labeling apparatus for 10s, the samples were incubated at 37°C for 20 min. An alkaline solution was then added to each well. OD values were measured using an enzyme labeling apparatus. The concentrations of alanine aminotransferase (ALT) and aspartate aminotransferase (AST) in the blood of rats in each group were calculated after the construction of standard curves were made respectively.

Measurement of Blood Renal Function

After 12 h of CLP, the upper layer of serum was collected using the same method described above. Enzyme solutions A and B were added sequentially. The optical density (OD) was measured using an enzyme labeling apparatus. The concentration of Crea in the blood of rats in each group was calculated after obtaining a standard curve. Other serum was taken. An enzyme working solution, color developer, and alkaline sodium hypochlorite were added sequentially. The optical density (OD) was measured using an enzyme labeling apparatus. The concentration of urea in the blood of rats in each group was calculated using a standard curve.

Blood D-Lactic Acid Content Detection

After 12 h of CLP, enzyme work-up and termination solutions were added according to the manufacturer's instructions. The OD value was determined colorimetrically at a wavelength of 530 nm. A standard curve was constructed to calculate the d-lactic acid concentration.

Molecular Docking Technique

AutoDockTools-1.5.6 software (The Molecular Graphics Laboratory, Scripps Research Institute, La Jolla, CA, USA) was used for the molecular docking analysis. Prior to docking, PyMol 2.6 (Pennsylvania), (USA) was used to process all the receptor proteins. For docking, the global search detail was set to 20 and all other parameters were set by default. The highest-scoring conformations were considered for docking as combined conformations. Finally, PyMol 2.6 and OpenBabel Transforming Molecular Structures (Pennsylvania, USA) were used to visually analyze the docking results.

Immunofluorescence and Immunohistochemical Staining

For immunofluorescence, cells were fixed with 4% paraformaldehyde, permeabilized with 0.1% Triton for 5 min, and then sealed with 5% BSA for 1 h. NLRP3 and GSDMD primary antibodies were incubated overnight at 4°C. The sections were then stained with a secondary antibody (1:200) for 30 min, washed with PBS, re-stained with DAPI for 10 min, and randomly photographed under a fluorescence microscope. Paraffin sections were subjected to immunohistochemical staining, and the slices were oven-baked at 60°C for 1 h. Then, the paraffin sections were deparaffinized in water and antigenically repaired. Endogenous peroxidase and serum were used as blocks. Primary antibodies against TRX1, NLRP3, and GSDMD were added, followed by secondary antibodies. DAB was used to develop color. Hematoxylin was used to re-stain the cell nuclei and the cells were observed under a microscope.

Mitochondrial Morphology and ROS Level Determination

IECs were inoculated into Petri dishes and incubated with Mito-tracker (1:10000) for 30 min at 37°C. Mitochondrial morphology and mitochondrial ROS levels were observed using a confocal laser scanning microscope (CLSM).

Western Blot

Cell level: 3~5 generations of intestinal epithelial cells were collected until 80% fusion, and then 1 µg/mL LPS, 5 mmol/L ATP, and 10 µmol/L drugs were added. Cells were collected from each group. Animal level: SD rats were fixed by intraperitoneal anesthesia and the abdomen was opened. A small number of intestinal segments were intercepted and the surfaces of the blood stains were rinsed with ice-cold PBS solution. Proteins were extracted separately and the gels were

electrophoresed. Protein strips were transferred onto polyvinylidene difluoride (PVDF) membranes. 5% skimmed milk powder was blocked for 1 h. Antibodies specific for the antigen to be tested were added and incubated overnight at 4°C, including TRX1, NLRP3, Caspase11, and GSDMD. The secondary antibody was then incubated for 1 h, scanned, and imaged using a chemiluminescence imaging analyzer. The strips were analyzed using the ImageJ software to detect the expression of each group of proteins. The bands were analyzed using ImageJ software to detect protein expression in each group.⁴⁵

CCK 8 Experiment

After the IECs were cultured in 96-well plates for 48 h, the medium in each well was carefully aspirated. The drug was added to each well and the same volume of medium was added to the blank group. The culture was incubated for 12 h. The liquid in the wells was carefully aspirated and 10 μ L of CCK-8 solution was added to each well for 2 h. The absorbance was recorded at 450 nm using an enzyme labelling apparatus and the cell survival rate was calculated.

Statistical Analysis

SPSS 28.0 (SPSS Inc., Chicago, Illinois, USA) was used for data analysis. Data are presented as the mean \pm standard deviation of at least three independent experiments. One-way analyses were performed using variance and post-hoc tests (S-N-K/LSD) to analyze the distinction between the experimental groups. $P < 0.05$ was considered statistically significant distinction.

Results

Characterization of Nano AC

The central peak of the spectrum was identified as 5,7-dihydroxy-4'-methoxyflavone (Acacetin) using a Liquid Chromatograph Mass Spectrometer (LCMS) (Figure 1A). Fourier Transform Infrared Spectroscopy (FTIR) showed characteristic absorption peaks: 3447 cm^{-1} corresponded to O-H and N-H stretching vibrations and 2960 cm^{-1} corresponded to C-H stretching vibrations. 1640 cm^{-1} , 1546 cm^{-1} , and 1450 cm^{-1} correspond to the amide I, II, and III bands of the protein, respectively. All these absorption peaks correspond to zein in the sample. The structure of acacetin is similar to that of flavonoids and is characterized by the C=C stretching vibration of the benzene ring near 1600 cm^{-1} (Figure 1B). Acacetin-loaded zein nanoparticles were uniformly dispersed with homogeneous size and spherical morphology. The drug was visible in the nanoparticles (Figure 1C). The average particle size of Nano AC was 17.18 ± 0.48 nm, PDI was 0.27 ± 0.1 , and the zeta potential was 11.5 ± 0.3 mV (Figure 1D-E). The uptake rate of Nano AC was higher than that of AC in intestinal epithelial cells, with a peak uptake time of 4 h. The average uptake rate of Nano AC was 95%, and the average uptake rate of AC was 81% (Figure 1F). Under a fluorescence microscope, the highest fluorescence intensity was observed at 4 h (Figure 2A). The mechanism of therapeutic effect of Nano AC on intestinal mucosa barrier after sepsis was presented (Figure 2B). The prepared solution of Nano AC was a homogeneous, stable, and creamy yellow liquid (Figure 2C). The standard curve of AC was $Y = 18879X + 61687$, the encapsulation rate of Nano AC was $87 \pm 0.5\%$, and the drug loading was $27 \pm 0.3\%$ (Figure 2D).

Protective Effect of Nano AC on Sepsis Rats

After treatment of non-nanoparticles, the rats did not die. It demonstrated that Non-nano was no impact on rats. SD rats underwent cecum ligation and perforation, and the 24 h survival rate was 0 in Sep group. Treatment of AC ameliorated the 24 h survival rate of sepsis rats, which was 25%. Nano AC further ameliorated the 24 h survival rate of sepsis rats, which was 62%. Rats survived up to 48 h in Nano AC group (Figure 3A-B). The inflammatory factors IL-1 β and IL-18 levels were elevated when the cells occurred pyroptosis.⁴⁶ Serum was taken from rats, and their levels of inflammatory factors were determined. Our results showed that IL-1 β and IL-18 levels were significantly elevated in Sep group, and the IL-1 β and IL-18 levels were reduced in both AC and Nano AC groups, with better results in Nano AC group. Nano AC group respectively reduced the levels by 63.6% and 52.9% compared to AC group (Figure 3C-D). AST and ALT are mainly distributed in hepatocytes, and the increased hepatocyte membrane permeability and its necrosis can increase

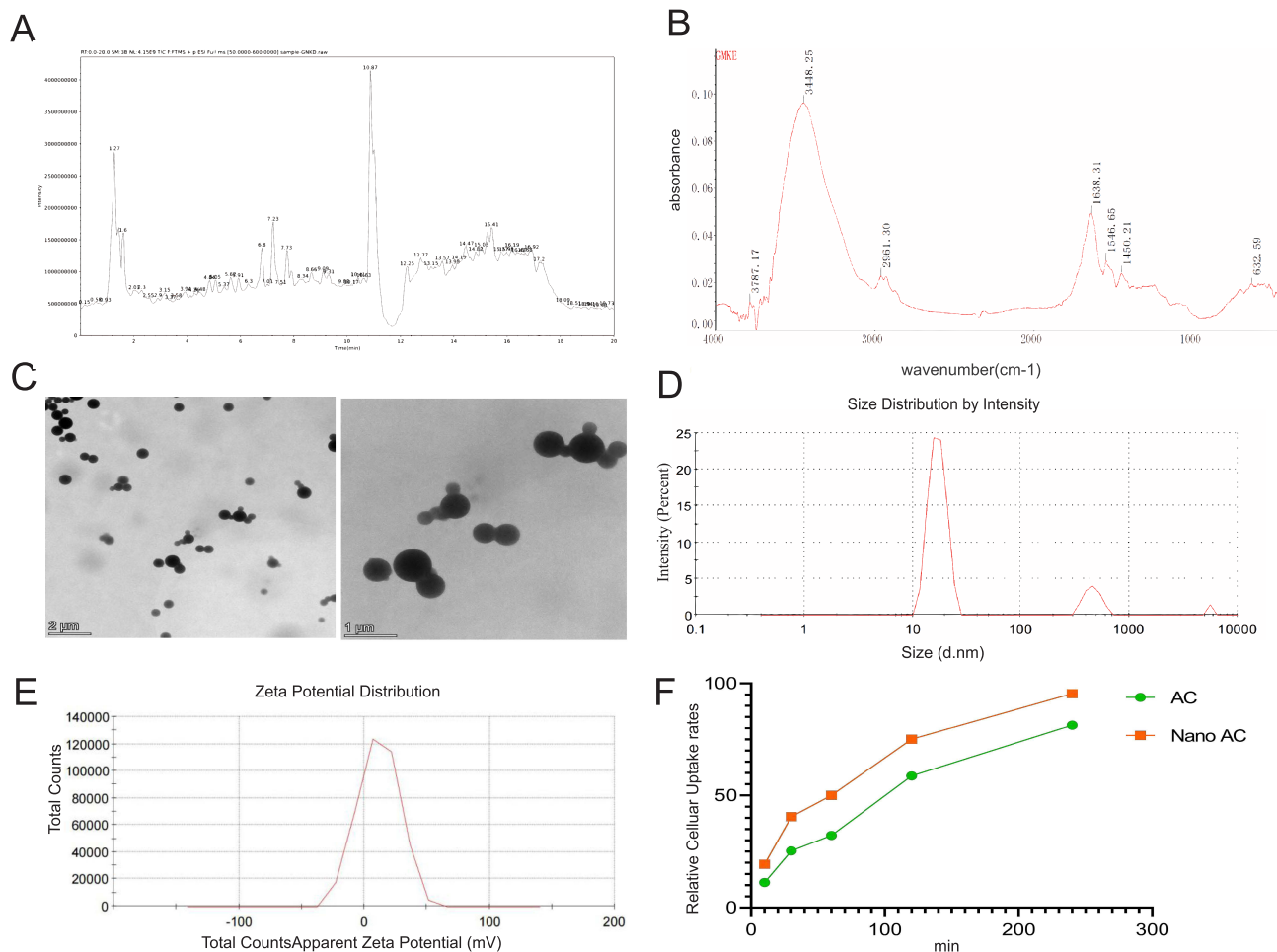


Figure 1 Characterization of Nano AC. **(A)** LC-MS spectrum of Nano AC. **(B)** Infrared spectroscopy of Nano AC. **(C)** Representative image of TEM of Nano AC. **(D)** Size distribution of Nano AC ($n=3$ independent experiments). **(E)** Zeta potential of Nano AC ($n=3$ independent experiments). **(F)** Uptake rates of AC and Nano AC by intestinal epithelial cells ($n=3$ independent experiments).

AST and ALT levels.⁴⁷ Crea and Urea are mainly secreted by the kidneys. Crea and Urea mainly reflect the function of renal injury.⁴⁸ The ELISA results showed that AST, ALT, Crea, and Urea levels were significantly elevated in Sep group, and the treatment of AC significantly ameliorated the liver and kidney functions of sepsis rats. Nano AC further respectively reduced AST, ALT, Crea, and Urea levels by 61%, 29.7%, 25.3%, and 55% compared with AC group (Figure 3E-H). Myocardial injury markers cardiac troponin T (cTnT) and cardiac troponin I (cTnI) were significantly elevated after CLP, which suggested altered myocardial function. The levels of cTnT and cTnI were reduced after AC treatment. Compared with AC group, treatment of Nano AC significantly reduced cTnT and cTnI levels by 58.8% and 57%, respectively. They showed that myocardial injury was significantly ameliorated (Figure 3I-J).

Nano AC Ameliorates Sepsis-Induced Intestinal Mucosal Injury by Modulating Pyroptosis Pathway

The effect of AC on TRX1 has not been reported in the literature, we used AutoDockTools-1.5.6 to analyze the interaction of AC with TRX1. In our study, AC inhibited the expression of TRX1 in intestinal epithelial cells, and the molecular docking technique simulated the binding ability of AC to TRX1. The affinity was predicted by calculating the binding energy. The binding energy was less than zero, indicating that the small molecule ligand had the ability to spontaneously bind to the large molecule receptor. When the binding energy is less than -5 kcal/mol, it indicates that the ligand binds well to the receptor.⁴⁹ In the present study, AC was bound to LYS-36, MET-37, and LYS-39 by conventional

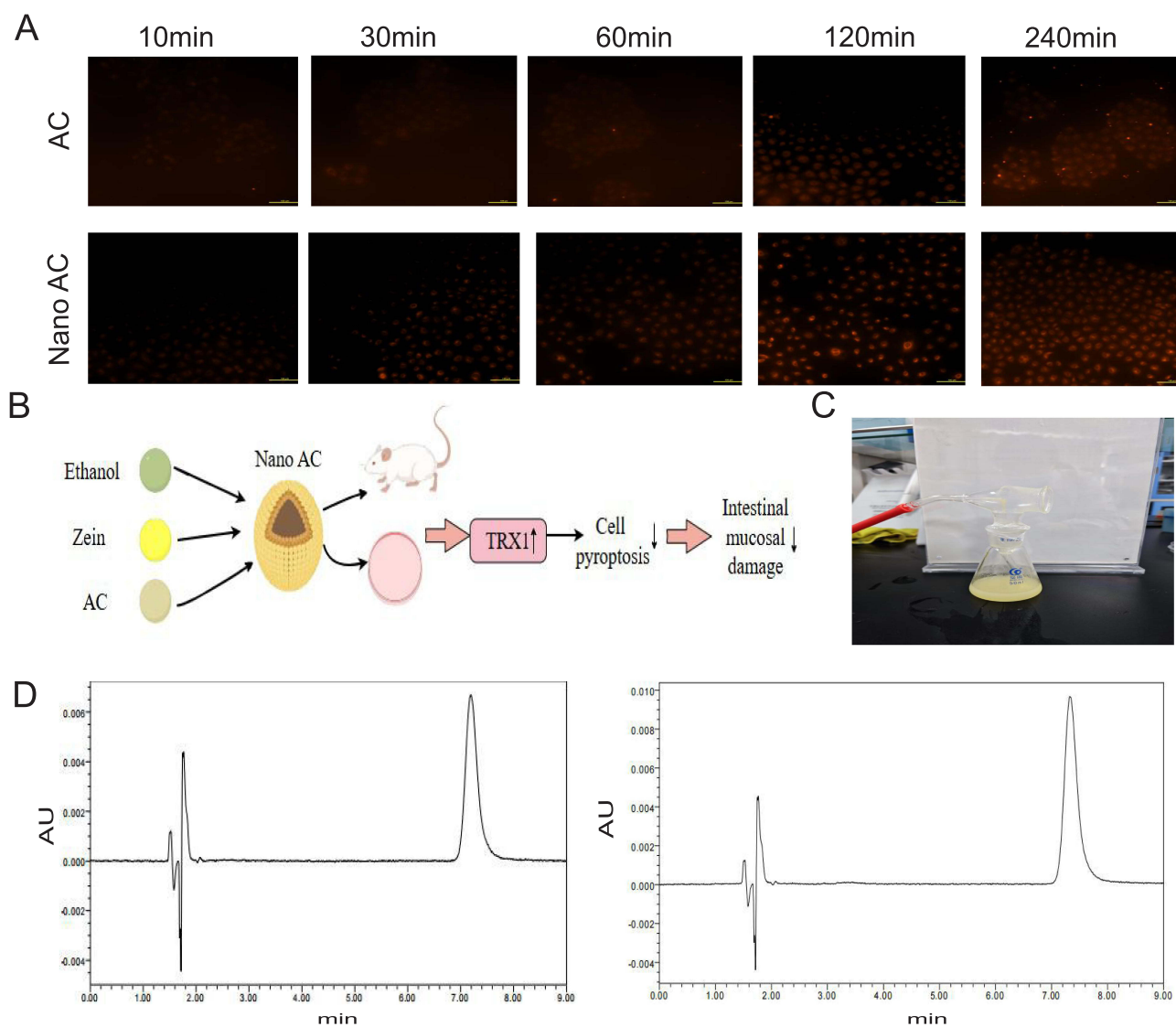


Figure 2 Characterization of Nano AC. (A) Uptake of rhodamine B by intestinal epithelial cells at each time point (n=3 independent experiments). (B) The diagram for the mechanism of therapeutic effect of Nano AC on intestinal mucosa barrier after sepsis. (C) The appearance of Nano AC. (D) The chromatogram of Nano AC encapsulation rate, drug loading.

hydrogen bonding; its maximum binding capacity to TRX1 was -6.82 kcal/mol, which showed a strong affinity (Figure 4A). Molecular docking techniques and experiments confirmed that AC inhibited TRX1 expression in intestinal epithelial cells. During sepsis, intestinal tract is regarded as a “motor” organ, and its mucosal epithelium acts as a protective barrier.⁵⁰ D-lactate is reflected intestinal barrier dysfunction. When intestinal mucosa is damaged, the level of D-lactic acid is increased in the blood.⁵¹ ELISA results showed that the level of D-lactic acid was significantly increased in Sep group. Then, treatment of AC significantly ameliorated the intestinal mucosal damage of sepsis rats. Nano AC further reduced the D-lactate level by 83.3% compared to the AC group (Figure 4B). Histological analysis of the intestinal tissues by hematoxylin and eosin (H&E) staining strongly supported the protective effect of Nano AC on intestinal tract. There was no pathological abnormality here in the intestinal tissues of Sham group, and small intestinal mucosa and submucosal interstitium were severely edematous with severe leukocyte infiltration in Sep group. Moreover, villi were disordered with severe structural damage. The intestinal tracts were significantly ameliorated in AC and Nano AC groups, and the improvement effect was more pronounced in Nano AC group (Figure 4C). The intestinal mucosal injury score was significantly higher in Sep group compared to Sham group. AC and Nano AC groups significantly reduced the intestinal mucosal injury score, which was lower in Nano AC group compared to AC group (Figure 4E). In

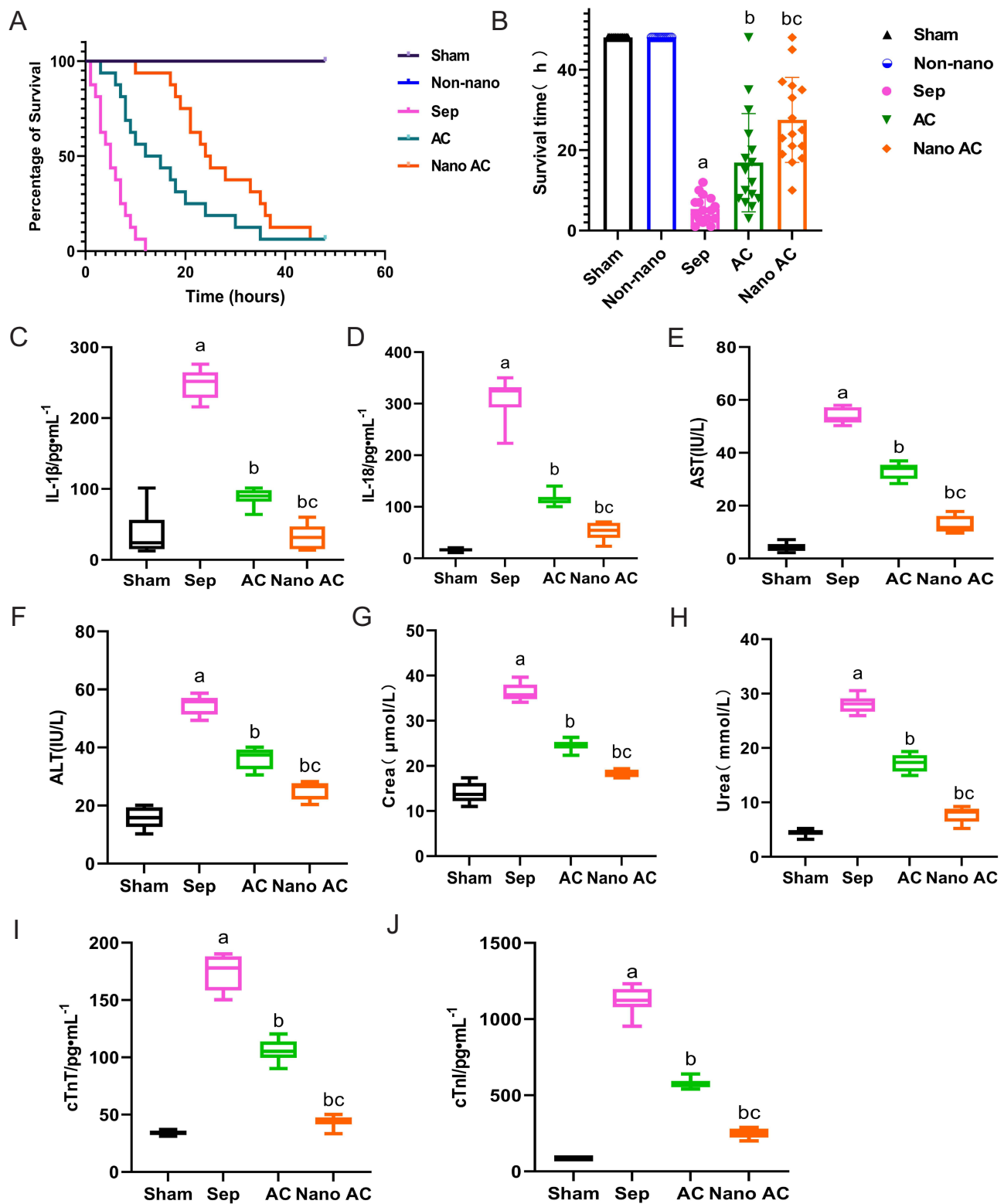


Figure 3 Protective Effect of Nano AC on Sepsis Rats. **(A)** Survival rate. **(B)** Survival time of each group (n=16 per group). Effects of Nano AC on **(C)** IL-1 β , **(D)** IL-18 and **(E)** AST **(F)** ALT, **(G)** Crea, **(H)** Urea, **(I)** cTnT and **(J)** cTnl level (n=8 per group). ^aP<0.05, compared with Sham group or Control group. ^bP<0.05, compared with Sep group or LPS group. ^cP<0.05, compared with AC group.

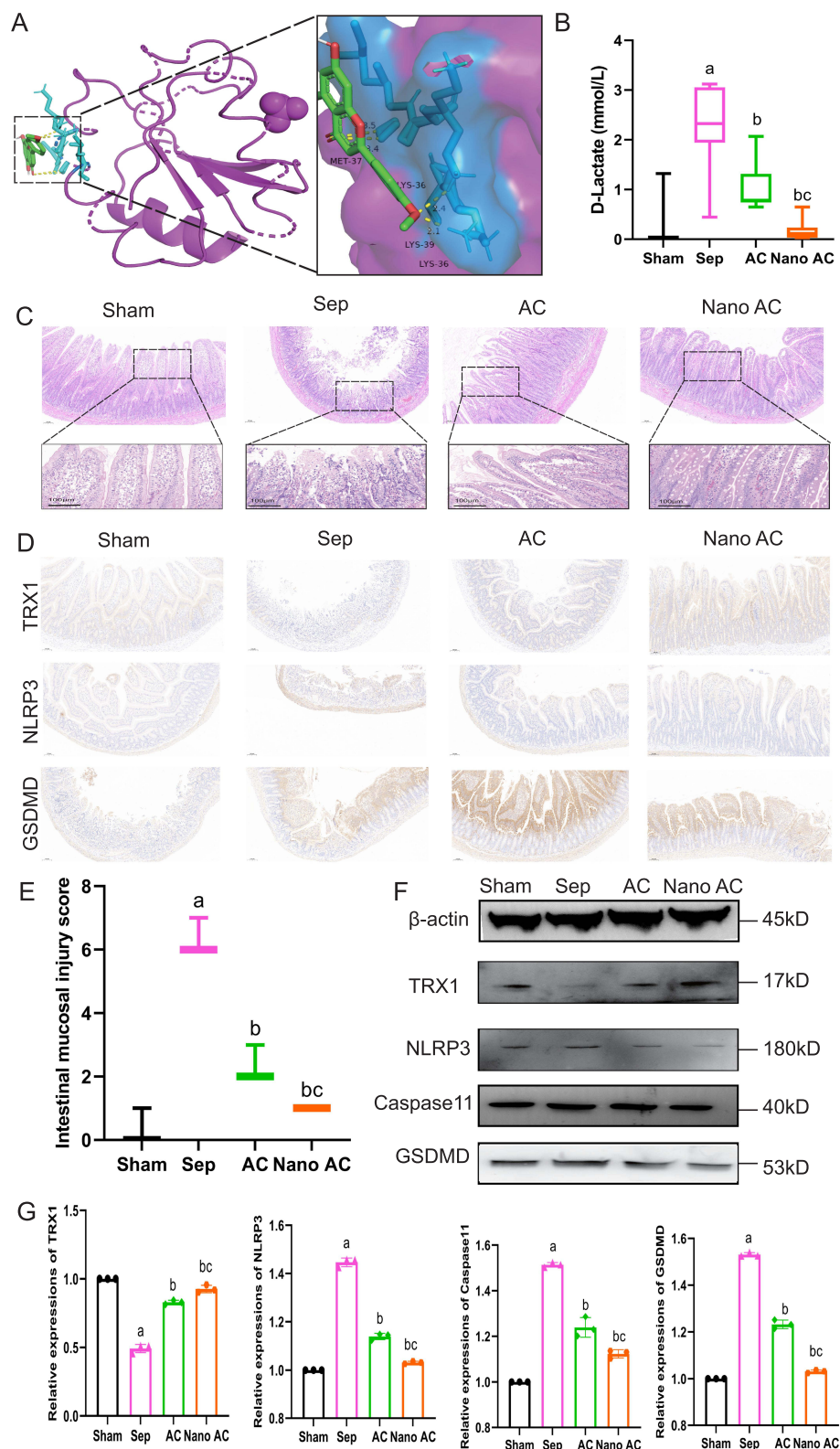


Figure 4 Nano AC ameliorates sepsis-induced intestinal mucosal injury by modulating pyroptosis pathway. **(A)** molecular docking. **(B)** Effects of Nano AC on D-lactic acid level (n=8 per group). **(C)** Representative microphotographs of HE staining in intestine (n=3 per group). **(D)** TRX1, NLRP3 and GSDMD representative microphotographs of immunohistochemical staining in intestine (n=3 independent experiments). **(E)** Intestinal mucosal injury score (n=3 per group). **(F)** Western blot of TRX1, NLRP3, Caspase11 and GSDMD in intestinal tissues of rats after treated with Nano AC (n=3 independent experiments). **(G)** The relative expressions of TRX1, NLRP3, Caspase11 and GSDMD (n=3 independent experiments). ^aP<0.05, compared with Sham group or Control group. ^bP<0.05, compared with Sep group or LPS group. ^cP<0.05, compared with AC group.

the immunohistochemical staining results, it was found that there was an obvious positive expression of TRX1 and no obvious positive expression of NLRP3 and GSDMD in Sham group. There was no obvious positive expression of TRX1 with light coloring, but obvious positive expression of NLRP3 and GSDMD with dark coloring and brown coloring in Sep group. Compared with Sep group, the rate of TRX1-positive cells was increased, and the rates of NLRP3 and GSDMD positive cells were reduced in AC group. These phenomenon could be further ameliorated in the Nano AC group (Figure 4D). Western blot results showed that expression of TRX1 was reduced in Sep group, and expression of NLRP3, Caspase11, and GSDMD was elevated; AC and Nano AC could significantly increase expression of TRX1 and significantly reduce expression of NLRP3, Caspase11, and GSDMD (Figure 4F-G). These results implied that Nano AC plays a protective role in the intestines of sepsis rats through TRX1/NLRP3/Caspase11/GSDMD signaling pathway.

Nano AC Protects Mitochondrial Function and Up-Regulates TRX1 to Inhibit Pyroptosis

Intestinal epithelial cells (IEC) form a physicochemical barrier separating the intestinal lumen from the host's internal environment and are intensely involved in mucosal inflammatory reactions and intestinal immune responses. The morphology of mitochondria was further observed in IEC, and laser confocal microscopy was used. Our studies found that mitochondrial morphology was linear in Control and Non-nano group; after LPS stimulation, mitochondrial structure showed apparent fragmentation with short dots; the fragmented mitochondrial structure of mitochondria was ameliorated in AC and Nano AC group. These results suggested that Non-nano was no impact on intestinal epithelial cells; AC could ameliorate morphology of mitochondria because LPS stimulated mitochondrial changes, and the effect was better in Nano AC group (Figure 5A). The levels of mitochondrial ROS were elevated after LPS stimulation. However, mitochondrial ROS levels were reduced after AC treatment and they were even further reduced after Nano AC treatment (Figure 5B). To determine regulatory effect of AC on the NLRP3 pathway via TRX1, protein expression of TRX1, NLRP3, Caspase11, and GSDMD was extracted from intestinal epithelial cells. Western blot results showed that AC up-regulated expression of TRX1 and down-regulated expression of NLRP3, Caspase11, and GSDMD (Figure 5C and E). In the follow-up experiments, we added PX-12, an inhibitor of TRX1, which was used to explore whether the action of AC on TRX1 was involved in the NLRP3 pathway to inhibit cellular pyroptosis. CCK-8 assay was used to examine effect of Nano AC on the viability of intestinal epithelial cells. The viability was decreased in LPS group when compared with Control group. It was increased in AC group when compared with LPS group and significantly increased in Nano AC group (Figure 5D). Immunofluorescence staining results showed that expression of NLRP3 and GSDMD was less in Control group and increased after LPS stimulation. In addition, their expression was decreased after AC and Nano AC treatments, and effect of Nano AC was more significant. On the contrary, expression of NLRP3 and GSDMD increased again after the addition of TRX1 inhibitor (PX-12) (Figure 5F). Western blot results demonstrated that Nano AC inhibited NLRP3/Caspase11/GSDMD pathway, but this ability was blocked by the addition of TRX1 inhibitor (Figure 5G-I). These evidences suggested that Nano AC ameliorates intestinal mucosal injury by protecting mitochondrial function and inhibiting intestinal epithelial cell pyroptosis through up-regulation TRX1 to inhibit NLRP3/Caspase11/GSDMD signal.

Discussion

Sepsis is a global health problem and a leading cause of death owing to infection.⁵² Recent studies have shown that the relationship between systemic sepsis and loss of intestinal barrier function has become a noteworthy area in clinical and preclinical research, and intestinal barrier dysfunction aggravates the severity and progression of sepsis.⁵³ The protection of intestinal mucosa is essential as a physicochemical barrier. The current study demonstrated the protective effects of Nano AC on the intestinal mucosal barrier in sepsis rats. Pyroptosis is an essential event in the gut that occurs during sepsis. The induction of pyroptosis depends on Caspase-11 activity in sepsis mice.^{54–56} NLRP3 interacted with Caspase-11. Notably, cleavage of GSDMD causes release of the functional gasdermin-N structural domain by active Caspase-1/4/5/11. The released structural domain subsequently forms pores in the membrane, which promote the active release of inflammatory cytokines and intracellular components.⁵⁷

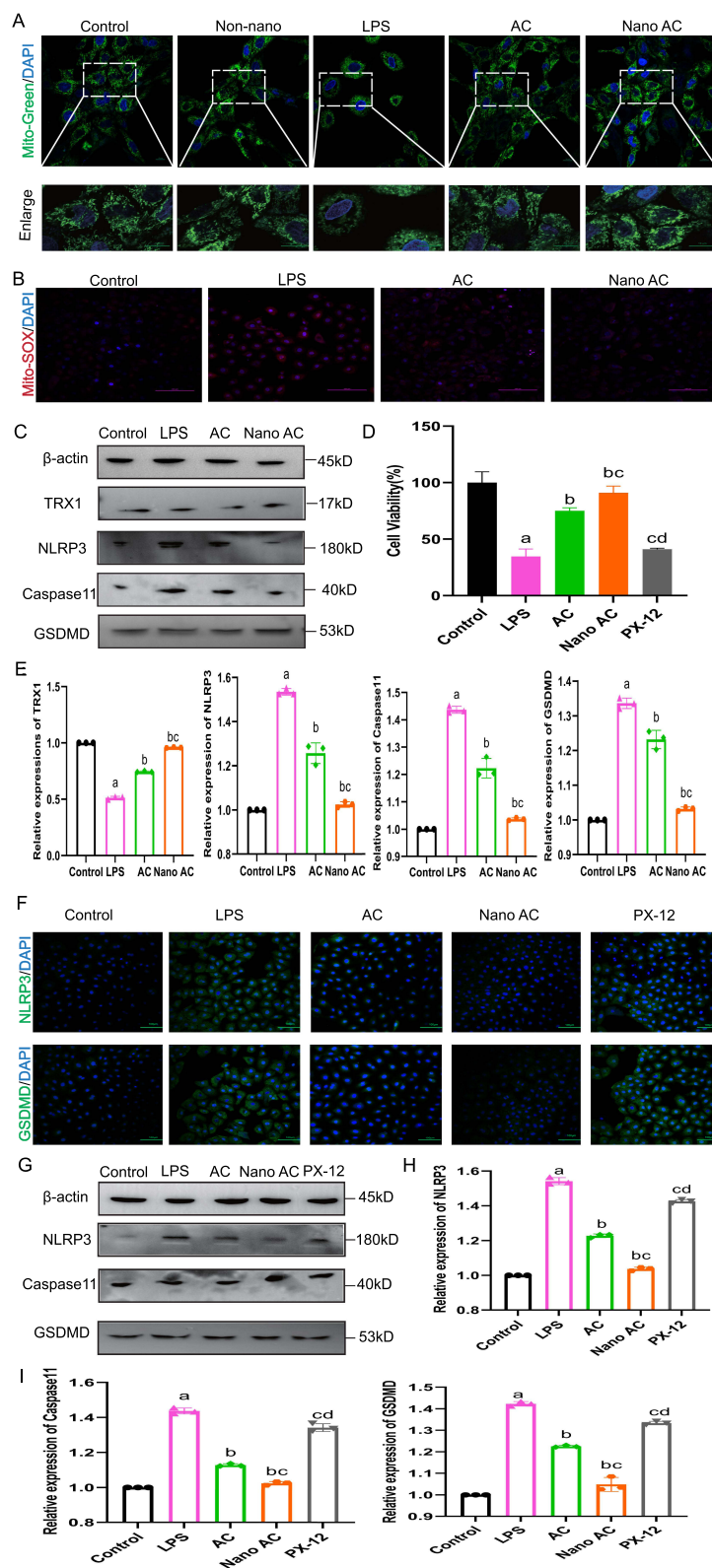


Figure 5 Nano AC protects mitochondrial function and up-regulates TRX1 to inhibit pyroptosis. **(A)** Mitochondrial morphology (n=3 independent experiments). **(B)** The effect of Nano AC on Mito-SOX of intestinal epithelial cells (n=3 independent experiments). **(C)** Western blot of TRX1, NLRP3, Caspase I and GSDMD in intestinal cells after treated with Nano AC (n=3 independent experiments). **(D)** The effect of Nano AC on cell viability (n=6 independent experiments). **(E)** The relative expressions of TRX1, NLRP3, Caspase I and GSDMD in intestinal cells (n=3 independent experiments). **(F)** Representative immunofluorescence image of NLRP3 and GSDMD of intestinal epithelial cell (n=3 independent experiments). **(G)** The effect of Nano PTL on the expression of NLRP3, Caspase I and GSDMD after adding TRX1 inhibitor (n=3 independent experiments). **(H-I)** The relative expressions of NLRP3, Caspase I and GSDMD (n=3 independent experiments). ^aP<0.05, compared with Sham group or Control group. ^bP<0.05, compared with Sep group or LPS group. ^cP<0.05, compared with AC group. ^dP<0.05, compared with Nano AC group.

Previous studies have found that AC alleviates dextran sodium sulfate-induced colitis by inhibiting macrophage inflammatory responses and reversing intestinal flora dysbiosis in mice.⁵⁸ Previous studies have not reported the role of AC in regulating TRX1 and the upstream regulatory proteins of NLRP3/Caspase-11/GSDMD in sepsis rats. In the present study, PX-12 was used to show that TRX1 is essential for the mechanism of AC in regulating sepsis pyroptosis. In addition, molecular docking techniques showed the interaction between AC and TRX1. Our study demonstrated that AC inhibits LPS-induced pyroptosis in intestinal epithelial cells by upregulating TRX1 expression. The expression of NLRP3/Caspase-11/GSDMD increased in Sep group. In contrast, NLRP3 expression was decreased after AC treatment. AC inhibited the expression of Caspase-11 and GSDMD in turn, and the effect of Nano AC became more obvious. We observed that AC and Nano AC increased cell viability in the CCK8 assay. This suggests that the protective effect of Nano AC may be via inhibition of the NLRP3 pathway in the intestinal mucosa of sepsis rats, which restrained cells from pyroptosis.

More and more evidence demonstrates that herbal medicines and their extracts play essential roles in treatment of inflammatory diseases.^{59,60} AC is a natural flavonoid compound with multiple therapeutic potentials in oxidative stress, inflammation, cancer, cardiovascular disease, and infection.⁶¹ Previous studies have found that AC inhibits cardiomyocyte apoptosis by suppressing the reduction of endogenous antioxidants and has a significant therapeutic effect on ischemia reperfusion-induced myocardial injury.⁶² However, due to the low solubility and short biological half-life of AC, its clinical application is limited. Therefore, the synthesis of Nano AC was considered. Protein-based biomaterials have outstanding research value, which is characterized by features such as high drug binding capacity, biodegradability, easy accessibility, and large surface area.⁶³ We utilized zein as carriers while retaining various pharmacological activities of AC. Zein has no cytotoxicity, high regenerability, and drug binding capacity as a nanocarrier.⁶⁴ Moreover, zein is an amphiphilic protein containing a high percentage of hydrophobic amino acids.⁶⁵ The method ameliorates the solubility and cell uptake percentage of AC. Our results show that AC is a promising drug candidate for clinical applications. We synthesized Nano AC, which elevated cellular uptake of the drug with an average particle size of 17.18 nm and a zeta potential of 11.5 mV. Among other nanomaterials, researchers prepared broad-spectrum reactive oxygen scavenging polysaccharide β -cyclodextrin (TPCD) with an anti-atherosclerotic effect, which was used to nano-therapeutically treat apolipoprotein e-deficient (ApoE^{-/-}) mice.⁶⁶ Oral administration of nanosized curcumin can be used as a complementary treatment for gingivitis and mild periodontitis due to its anti-inflammatory effects.⁶⁷ The anti-inflammatory activity of nanosized peroxidase was significantly higher than aspirin in colon carcinogenesis associated with bacteria and inflammation.⁶⁸ In our study, we demonstrated that Nano AC ameliorated the 24 h survival rate of sepsis rats which was 62%. Nano AC respectively reduced AST, ALT, Crea, and Urea levels by 76.1%, 53.6%, 49.4%, and 72.4% compared with Sep group protecting liver and kidney function. It significantly reduced cTnT and cTnI levels by 75% and 77.8% protecting myocardial injury, but also intestinal mucosal injury. In order to observe the protective mechanism of Nano AC on intestinal mucosa, we measured the intestinal mucosal injury damage scores, which found that Nano AC reduced the intestinal mucosal injury damage scores in vivo experiments. Then we replicated the sepsis model by using LPS, which found that Nano AC up-regulated TRX1 inhibited the NLRP3/Caspase-11/GSDMD signaling pathway in turn, an effect that was reversed by PX-12 in vitro experiments. These results further confirmed that Nano AC reduces sepsis-associated inflammatory responses and the role of Nano AC in intestinal protective effects via TRX1/NLRP3/Caspase-11/GSDMD signaling pathway.

Previous studies have shown that mitochondrial dysfunction plays a crucial role in multi-organ dysfunction after critical illness, and the degree of mitochondrial dysfunction determines the prognosis of patients.⁶⁹ In our experiments, mitochondrial morphology was further observed, and Nano AC restored the mitochondrial morphological changes induced by LPS stimulation. Research has previously demonstrated that dysfunctional mitochondria induce and enhance inflammatory responses through production of mitochondrial ROS, and activation of NLRP3 can be via mt ROS.⁷⁰ TRX1 has roles of scavenging mt ROS, we found that Nano AC reduced mt ROS level and protected mitochondrial function in intestinal epithelial cells.

However, our studies have some limitations. Firstly, vivo studies are necessary to confirm Nano AC molecular targets and TRX1 knockout mice should be used to assess the role of Nano AC. In addition, computerized molecular docking showed an interaction between TRX1 and AC, which needs to be further verified by specific experiments.

Conclusion

Our studies indicated that Nano AC has a protective effect against sepsis-induced intestinal mucosal injury and that Nano AC can up-regulate TRX1 to inhibit the NLRP3/Caspase-11/GSDMD signaling pathway. Our findings provide evidence that Nano AC targets regulation TRX1. Therefore, Nano AC may be a future candidate for intestinal mucosal injury in sepsis.

Abbreviations

AC, acacetin; Nano AC, Nano acacetin; CLP, cecum ligation and perforation; LPS, lipopolysaccharide; TRX1, thioredoxin reductase 1; NLRP3, NOD-like receptor protein 3 inflammasome; Caspase-11, cysteinyl aspartate specific proteinase-11; GSDMD, Gasdermin D; DMSO, Dimethyl sulfoxide; GaIN, galactosamine; iNOS, inducible nitric oxide synthase; COX-2, cyclooxygenase 2; TPA, 12-O-tetradecanoylphorbol-13-acetate; IL-1 β , interleukin 1 β ; IL-18, interleukin 18; ROS, reactive oxygen species; DSS, dextran sodium sulfate; LCMS, Liquid Chromatograph Mass Spectrometer; ZP, zeta potential; PDI, polydispersity index; ATP, adenosine-triphosphate; cTnT, cardiac troponin T; cTnI, cardiac troponin I; ALT, alanine aminotransferase; AST, aspartate aminotransferase; IEC, intestinal epithelial cell; mt ROS, mitochondrial ROS; PVDF, polyvinylidene difluoride; TPCD, polysaccharide β -cyclodextrin.

Data Sharing Statement

The raw data of this study are available from the corresponding author on reasonable request.

Ethics Approval and Consent to Participate

The Ethics Committee of the Clinical Medical School, Qinghai University, approved the ethics and protocols for animal experiments.

Author Contributions

All authors made a significant contribution to the work reported, whether in the conception, study design, execution, acquisition of data, analysis, and interpretation, or in all these areas, took part in drafting, revising, or critically reviewing the article; gave final approval of the version to be published; have agreed on the journal to which the article has been submitted; and agree to be accountable for all aspects of the work.

Funding

This study was supported by the Qinghai Province Applied Basic Research Program of China (No.2022-ZJ-754).

Disclosure

The authors report no conflicts of interest in this work.

References

1. Hamers L, Kox M, Pickkers P. Sepsis-induced immunoparalysis: mechanisms, markers, and treatment options. *Min Anesthesiol*. 2014;81: 426–39.
2. Liu D, Huang SY, Sun JH, et al. Sepsis-induced immunosuppression: mechanisms, diagnosis and current treatment options. *Mil Med Res*. 2022;9(1):56. doi:10.1186/s40779-022-00422-y
3. Chen W, Wang Y, Zhou T, Xu Y, Zhan J, Wu J. CXCL13 is involved in the lipopolysaccharide-induced hyperpermeability of umbilical vein endothelial cells. *Inflammation*. 2020;43(5):1789–1796. doi:10.1007/s10753-020-01253-6
4. Gyawali B, Ramakrishna K, Dharamoon AS. Sepsis: the evolution in definition, pathophysiology, and management. *SAGE Open Med*. 2019;7:205031211983504. doi:10.1177/2050312119835043
5. Cawcutt KA, Peters SG. Severe sepsis and septic shock: clinical overview and update on management. *Mayo Clin Proc*. 2014;89(11):1572–1578. doi:10.1016/j.mayocp.2014.07.009
6. Kumar V. Pulmonary innate immune response determines the outcome of inflammation during pneumonia and sepsis-associated acute lung injury. *Front Immunol*. 2020;11:1722. doi:10.3389/fimmu.2020.01722
7. Wang YF, Li JW, Wang DP, Jin K, Hui JJ, Xu HY. Anti-hyperglycemic agents in the adjuvant treatment of sepsis: improving intestinal barrier function. *Drug Des Dev Ther*. 2022;16:1697–1711. doi:10.2147/DDDT.S360348
8. Hu Q, Ren H, Li G, et al. STING-mediated intestinal barrier dysfunction contributes to lethal sepsis. *EBioMedicine*. 2019;41:497–508. doi:10.1016/j.ebiom.2019.02.055
9. Chen F, Chu C, Wang X, et al. Hesperetin attenuates sepsis-induced intestinal barrier injury by regulating neutrophil extracellular trap formation via the ROS/autophagy signaling pathway. *Food Funct*. 2023;14(9):4213–4227. doi:10.1039/D2FO02707K

10. Shang L, Li J, Zhou F, Zhang M, Wang S, Yang S. MiR-874-5p targets VDR/NLRP3 to reduce intestinal pyroptosis and improve intestinal barrier damage in sepsis. *Int Immunopharmacol.* **2023**;121:110424. doi:10.1016/j.intimp.2023.110424
11. Cao Y, Tan YJ, Huang D. Anti-inflammation mechanisms of flavones are highly sensitive to the position isomers of flavonoids: acacetin vs biochanin A. *J Agric Food Chem.* **2024**;72(41):22939–51. doi:10.1021/acs.jafc.4c05060
12. Singh S, Gupta P, Meena A, Luqman S. Acacetin, a flavone with diverse therapeutic potential in cancer, inflammation, infections and other metabolic disorders. *Food Chem Toxicol.* **2020**;145:111708. doi:10.1016/j.fct.2020.111708
13. Ouyang Y, Rong Y, Wang Y, et al. A systematic study of the mechanism of acacetin against sepsis based on network pharmacology and experimental validation. *Front Pharmacol.* **2021**;12:683645. doi:10.3389/fphar.2021.683645
14. Liou CJ, Wu SJ, Chen LC, Yeh KW, Chen CY, Huang WC. Acacetin from traditionally used *saussurea involucreta* Kar. et Kir. suppressed adipogenesis in 3T3-L1 adipocytes and attenuated lipid accumulation in obese mice. *Front Pharmacol.* **2017**;8:589. doi:10.3389/fphar.2017.00589
15. Cho HI, Park JH, Choi HS, et al. Protective mechanisms of acacetin against d-galactosamine and lipopolysaccharide-induced fulminant hepatic failure in mice. *J Nat Prod.* **2014**;77(11):2497–2503. doi:10.1021/np500537x
16. Pan MH, Lai CS, Wang YJ, Ho CT. Acacetin suppressed lps-induced up-expression of iNOS and COX-2 in murine macrophages and tpa-induced tumor promotion in mice. *Biochem Pharmacol.* **2006**;72(10):1293–1303. doi:10.1016/j.bcp.2006.07.039
17. Sun LC, Zhang HB, Gu CD, et al. Protective effect of acacetin on sepsis-induced acute lung injury via its anti-inflammatory and antioxidative activity. *Arch Pharmacol Res.* **2018**;41(12):1199–1210. doi:10.1007/s12272-017-0991-1
18. Wang Y, Chen Q, Huang X, Yan X. Acacetin-loaded microemulsion for transdermal delivery: preparation, optimization and evaluation. *Pharm Biol.* **2023**;61(1):790–798. doi:10.1080/13880209.2023.2207597
19. Elzoghby AO, Elgohary MM, Kamel NM. Chapter six - implications of protein- and peptide-based nanoparticles as potential vehicles for anticancer drugs. In: Donev R, editor. *Advances in Protein Chemistry and Structural Biology. Vol 98. Protein and Peptide Nanoparticles for Drug Delivery.* Academic Press; **2015**:169–221. doi:10.1016/bs.apcsb.2014.12.002
20. Elzoghby AO, Vranic BZ, Samy WM, Elgindy NA. Swellable floating tablet based on spray-dried casein nanoparticles: near-infrared spectral characterization and floating matrix evaluation. *Int J Pharm.* **2015**;491(1–2):113–122. doi:10.1016/j.ijpharm.2015.06.015
21. Sajjadi M, Nasrollahzadeh M, Ghafari H. Functionalized chitosan-inspired (nano)materials containing sulfonic acid groups: synthesis and application. *Carbohydr Polym.* **2024**;343:122443. doi:10.1016/j.carbpol.2024.122443
22. André De Almeida Campos L, Francisco Silva Neto A, Cecília Souza Noronha M, Ferreira De Lima M, Macário Ferro Cavalcanti I, Stela Santos-Magalhães N. Zein nanoparticles for drug delivery: preparation methods and biological applications. *Int J Pharm.* **2023**;635:122754. doi:10.1016/j.ijpharm.2023.122754
23. Wang Y, Padua GW. Nanoscale characterization of zein self-assembly. *Langmuir.* **2012**;28(5):2429–2435. doi:10.1021/la204204j
24. Suzuki YA, Lopez V, Lönnnerdal B. Lactoferrin. *Cell Mol Life Sci.* **2005**;62(22):2560–2575. doi:10.1007/s00018-005-5371-1
25. Wang G, Han J, Meng X, et al. Zein-based nanoparticles improve the therapeutic efficacy of a TrkB agonist toward alzheimer's disease. *ACS Chem Neurosci.* **2023**;14(17):3249–3264. doi:10.1021/acscchemneuro.3c00401
26. Kesavardhana S, Malireddi RKS, Kanneganti TD. Caspases in cell death, inflammation, and pyroptosis. *Annu Rev Immunol.* **2020**;38(1):567–595. doi:10.1146/annurev-immunol-073119-095439
27. Gaidt MM, Hornung V. Pore formation by GSDMD is the effector mechanism of pyroptosis. *EMBO J.* **2016**;35(20):2167–2169. doi:10.15252/embj.201695415
28. Yao L, Cai H, Fang Q, et al. Piceatannol alleviates liver ischaemia/reperfusion injury by inhibiting TLR4/NF-κB/NLRP3 in hepatic macrophages. *Eur J Pharmacol.* **2023**;960:176149. doi:10.1016/j.ejphar.2023.176149
29. Chen L, Zhao Y, Lai D, et al. Neutrophil extracellular traps promote macrophage pyroptosis in sepsis. *Cell Death Dis.* **2018**;9(6):597. doi:10.1038/s41419-018-0538-5
30. Jorgensen I, Miao EA. Pyroptotic cell death defends against intracellular pathogens. *Immunol Rev.* **2015**;265(1):130–142. doi:10.1111/imr.12287
31. Miao R, Jiang C, Chang WY, et al. Gasdermin D permeabilization of mitochondrial inner and outer membranes accelerates and enhances pyroptosis. *Immunity.* **2023**;56(11):2523–2541.e8. doi:10.1016/j.immuni.2023.10.004
32. Huang Y, Zhou JH, Zhang H, et al. Brown adipose TRX2 deficiency activates mtDNA-NLRP3 to impair thermogenesis and protect against diet-induced insulin resistance. *J Clin Invest.* **2022**;132(9):e148852. doi:10.1172/JCI148852
33. Kim SM, Park YJ, Shin MS, et al. Acacetin inhibits neuronal cell death induced by 6-hydroxydopamine in cellular Parkinson's disease model. *Bioorg Med Chem Lett.* **2017**;27(23):5207–5212. doi:10.1016/j.bmcl.2017.10.048
34. Jin P, Zhou Q, Xi S. Low-dose arsenite causes overexpression of EGF, TGFα, and HSP90 through Trx1-TXNIP-NLRP3 axis mediated signaling pathways in the human bladder epithelial cells. *Ecotoxicol Environ Saf.* **2022**;247:114263. doi:10.1016/j.ecoenv.2022.114263
35. Abbate A, Toldo S, Marchetti C, Kron J, Van Tassell BW, Dinarello CA. Interleukin-1 and the inflammasome as therapeutic targets in cardiovascular disease. *Circ Res.* **2020**;126(9):1260–1280. doi:10.1161/CIRCRESAHA.120.315937
36. Moretti J, Jia B, Hutchins Z, et al. Caspase-11 interaction with NLRP3 potentiates the noncanonical activation of the NLRP3 inflammasome. *Nat Immunol.* **2022**;23(5):705–717. doi:10.1038/s41590-022-01192-4
37. Jia Y, Cui R, Wang C, et al. Metformin protects against intestinal ischemia-reperfusion injury and cell pyroptosis via TXNIP-NLRP3-GSDMD pathway. *Redox Biol.* **2020**;32:101534. doi:10.1016/j.redox.2020.101534
38. Hou Y, Wang Y, He Q, et al. Nrf2 inhibits NLRP3 inflammasome activation through regulating Trx1/TXNIP complex in cerebral ischemia reperfusion injury. *Behav Brain Res.* **2018**;336:32–39. doi:10.1016/j.bbr.2017.06.027
39. Tsolaki E, Stocker MW, Healy AM, Ferguson S. Formulation of ionic liquid APIs via spray drying processes to enable conversion into single and two-phase solid forms. *Int J Pharm.* **2021**;603:120669. doi:10.1016/j.ijpharm.2021.120669
40. Bie BJ, Zhao XR, Yan JR, Ke XJ, Liu F, Yan GP. Dextran fluorescent probes containing sulfadiazine and rhodamine B groups. *Molecules.* **2022**;27(19):6747. doi:10.3390/molecules27196747
41. Zhu Y, Kuang L, Wu Y, et al. Protective effects of inhibition of mitochondrial fission on organ function after sepsis. *Front Pharmacol.* **2021**;12:712489. doi:10.3389/fphar.2021.712489
42. Yamashita S, Suzuki T, Iguchi K, et al. Cardioprotective and functional effects of levosimendan and milrinone in mice with cecal ligation and puncture-induced sepsis. *Naunyn-Schmiedeberg's Arch Pharmacol.* **2018**;391(9):1021–1032. doi:10.1007/s00210-018-1527-z
43. Sun J, Ge X, Wang Y, Niu L, Tang L, Pan S. USF2 knockdown downregulates THBS1 to inhibit the TGF-β signaling pathway and reduce pyroptosis in sepsis-induced acute kidney injury. *Pharmacol Res.* **2022**;176:105962. doi:10.1016/j.phrs.2021.105962

44. Wenying S, Jing H, Ying L, Hui D. The role of TLR4/MyD88/NF- κ B in the protective effect of ulinastatin on the intestinal mucosal barrier in mice with sepsis. *BMC Anesthesiol.* 2023;23(1):414. doi:10.1186/s12871-023-02374-9
45. Huang N, Wei Y, Wang M, et al. Dachaihu decoction alleviates septic intestinal epithelial barrier disruption via PI3K/AKT pathway based on transcriptomics and network pharmacology. *J Ethnopharmacol.* 2025;337:118937. doi:10.1016/j.jep.2024.118937
46. Yao F, Jin Z, Zheng Z, et al. HDAC11 promotes both NLRP3/caspase-1/GSDMD and caspase-3/GSDME pathways causing pyroptosis via ERG in vascular endothelial cells. *Cell Death Discov.* 2022;8(1):112. doi:10.1038/s41420-022-00906-9
47. Sharma A, Verma AK, Kofron M, et al. Lipopolysaccharide reverses hepatic stellate cell activation through modulation of cMyb, small mothers against decapentaplegic, and CCAAT/enhancer-binding protein C/EBP transcription factors. *Hepatology.* 2020;72(5):1800–1818. doi:10.1002/hep.31188
48. De Loor J, Daminet S, Smets P, Maddens B, Meyer E. Urinary biomarkers for acute kidney injury in dogs. *J Vet Intern Med.* 2013;27(5):998–1010. doi:10.1111/jvim.12155
49. Rastelli G, Pinzi L. Molecular docking: shifting paradigms in drug discovery. *Int J Mol Sci.* 2019;20(18):4331. doi:10.3390/ijms20184331
50. Vinarov Z, Abdallah M, Agundez JAG, et al. Impact of gastrointestinal tract variability on oral drug absorption and pharmacokinetics: an UNGAP review. *Eur J Pharm Sci.* 2021;162:105812. doi:10.1016/j.ejps.2021.105812
51. Peoc'h K, Nuzzo A, Guedj K, Paugam C, Corcos O. Diagnosis biomarkers in acute intestinal ischemic injury: so close, yet so far. *Clin Chem Lab Med CCLM.* 2018;56(3):373–385. doi:10.1515/cclm-2017-0291
52. McBride MA, Patil TK, Bohannon JK, Hernandez A, Sherwood ER, Patil NK. Immune checkpoints: novel therapeutic targets to attenuate sepsis-induced immunosuppression. *Front Immunol.* 2021;11:624272. doi:10.3389/fimmu.2020.624272
53. Wang H, Zhang S, Zhao H, et al. Carbon monoxide inhibits the expression of proteins associated with intestinal mucosal pyroptosis in a rat model of sepsis induced by cecal ligation and puncture. *Med Sci Monit.* 2020;26:e920668–1–e920668–14. doi:10.12659/MSM.920668
54. Rühl S, Broz P. Caspase-11 activates a canonical NLRP3 inflammasome by promoting K⁺ efflux. *Eur J Immunol.* 2015;45(10):2927–2936. doi:10.1002/eji.201545772
55. Case CL, Kohler LJ, Lima JB, et al. Caspase-11 stimulates rapid flagellin-independent pyroptosis in response to Legionella pneumophila. *Proc Natl Acad Sci.* 2013;110(5):1851–1856. doi:10.1073/pnas.1211521110
56. Kayagaki N, Stowe IB, Lee BL, et al. Caspase-11 cleaves gasdermin D for non-canonical inflammasome signalling. *Nature.* 2015;526(7575):666–671. doi:10.1038/nature15541
57. Zhang W, Jiang H, Wu G, et al. The pathogenesis and potential therapeutic targets in sepsis. *MedComm.* 2023;4(6):e418. doi:10.1002/mco.2418
58. Ren J, Yue B, Wang H, et al. Acacetin ameliorates experimental colitis in mice via inhibiting macrophage inflammatory response and regulating the composition of gut microbiota. *Front Physiol.* 2021;11:577237. doi:10.3389/fphys.2020.577237
59. Ren Y, Qiao W, Fu D, et al. Traditional Chinese medicine protects against cytokine production as the potential immunosuppressive agents in atherosclerosis. *J Immunol Res.* 2017;2017(1):1–8. doi:10.1155/2017/7424307
60. Zhang J-L, Li W-X, Li Y, Wong M-S, Wang Y-J, Zhang Y. Therapeutic options of TCM for organ injuries associated with COVID-19 and the underlying mechanism. *Phytomedicine.* 2021;85:153297. doi:10.1016/j.phymed.2020.153297
61. Wang Y, Liu L, Ge M, Cui J, Dong X, Shao Y. Acacetin attenuates the pancreatic and hepatorenal dysfunction in type 2 diabetic rats induced by high-fat diet combined with streptozotocin. *J Nat Med.* 2023;77(3):446–454. doi:10.1007/s11418-022-01675-6
62. Liu H, Yang L, Wu HJ, et al. Water-soluble acacetin prodrug confers significant cardioprotection against ischemia/reperfusion injury. *Sci Rep.* 2016;6(1):36435. doi:10.1038/srep36435
63. Kimna C, Tamburaci S, Tihminlioglu F. Novel zein-based multilayer wound dressing membranes with controlled release of gentamicin. *J Biomed Mater Res B Appl Biomater.* 2019;107(6):2057–2070. doi:10.1002/jbm.b.34298
64. Elzoghby A, Freag M, Mamdouh H, Elkhodairy K. Zein-based nanocarriers as potential natural alternatives for drug and gene delivery: focus on cancer therapy. *Curr Pharm Des.* 2018;23(35):5261–5271. doi:10.2174/1381612823666170622111250
65. Paliwal R, Palakurthi S. Zein in controlled drug delivery and tissue engineering. *J Control Release.* 2014;189:108–122. doi:10.1016/j.jconrel.2014.06.036
66. Wang Y, Li L, Zhao W, et al. Targeted therapy of atherosclerosis by a broad-spectrum reactive oxygen species scavenging nanoparticle with intrinsic anti-inflammatory activity. *ACS Nano.* 2018;12(9):8943–8960. doi:10.1021/acsnano.8b02037
67. Malekzadeh M, Kia SJ, Mashaei L, Moosavi M-S. Oral nano-curcumin on gingival inflammation in patients with gingivitis and mild periodontitis. *Clin Exp Dent Res.* 2021;7(1):78–84. doi:10.1002/cre2.330
68. Al-Hazmi NE, Naguib DM. Nano-peroxidase a promising anti-inflammatory and antibacterial agent against bacteria and inflammation related to colorectal cancer. *J Gastrointest Cancer.* 2022;53(2):415–419. doi:10.1007/s12029-021-00626-w
69. Annesley SJ, Fisher PR. Mitochondria in Health and Disease. *Cells.* 2019;8(7):680. doi:10.3390/cells8070680
70. Zhou L, Yao M, Tian Z, et al. Echinacoside attenuates inflammatory response in a rat model of cervical spondylotic myelopathy via inhibition of excessive mitochondrial fission. *Free Radic Biol Med.* 2020;152:697–714. doi:10.1016/j.freeradbiomed.2020.01.014

International Journal of Nanomedicine

Publish your work in this journal

The International Journal of Nanomedicine is an international, peer-reviewed journal focusing on the application of nanotechnology in diagnostics, therapeutics, and drug delivery systems throughout the biomedical field. This journal is indexed on PubMed Central, MedLine, CAS, SciSearch®, Current Contents®/Clinical Medicine, Journal Citation Reports/Science Edition, EMBASE, Scopus and the Elsevier Bibliographic databases. The manuscript management system is completely online and includes a very quick and fair peer-review system, which is all easy to use. Visit <http://www.dovepress.com/testimonials.php> to read real quotes from published authors.

Submit your manuscript here: <https://www.dovepress.com/international-journal-of-nanomedicine-journal>

Dovepress
Taylor & Francis Group